J. Phys. B: At. Mol. Phys. **20** (1987) 3501-3514. Printed in the UK

Pulsed crossed-beam study of the ionisation of atomic hydrogen by electron impact

M B Shah, D S Elliott and H B Gilbody

Department of Pure and Applied Physics, The Queen's University of Belfast, Belfast BT7 1NN, UK

Received 26 January 1987

Abstract. A pulsed crossed-beam technique incorporating time of flight spectroscopy has been successfully developed and applied to measurements of the electron impact ionisation cross sections of atomic hydrogen in the range 14.6-4000 eV. The method has been derived from a crossed-beam coincidence technique used previously in this laboratory for proton impact studies of high accuracy. By substituting a pulsed proton beam for the pulsed electron beam in the present work, measured electron impact ionisation cross sections have been normalised by reference to known equivelocity proton impact cross sections for both ionisation and charge transfer. Our results resolve the discrepancy between earlier less accurate cross sections measured using the modulated crossed-beam technique. They provide a reliable check on the range of validity of theoretical predictions over a wide energy range.

1. Introduction

Continued interest in the simple ionisation process

$$e + H(1s) \rightarrow e + H^+ + e \tag{1}$$

stems partly from the search for adequate descriptions of the Coulomb three-body problem. While recent experimental studies of triple differential cross sections (cf the review by Weigold (1985)) can provide a sensitive test of theory, there is also a need for accurate total ionisation cross sections. These find direct application in fusion energy research and in astrophysics.

Previous studies of the total ionisation cross sections for (1) carried out by Fite and Brackmann (1958) in the range 17-750 eV and by Rothe *et al* (1962) in the range 100-750 eV were based on the modulated crossed-beam technique. In this approach, the primary beam of electrons is arranged to intersect a thermal energy beam of highly dissociated hydrogen which is chopped at a fixed frequency. The current due to slow protons arising from the process in question is distinguished from that due to collision products arising from interactions with the background gas by its specific frequency and phase. By comparing signals obtained from a mainly H atom beam with those from an H_2 beam, an ionisation cross section ratio $\sigma(H)/\sigma(H_2)$ can be obtained. Using values of $\sigma(H_2)$ previously measured by Tate and Smith (1932) using the beam-static-target approach, values of $\sigma(H)$ for (1) were then determined. Those obtained by Fite and Brackmann (1958) are about 27% larger than those of Rothe *et al* (1962) at 100 eV, the lowest energy in the range of overlap. A detailed comparison with theory is also precluded by the scatter of individual values of cross sections and large overall uncertainties.

0022-3700/87/143501+14$02.50

In the present work we have used a different experimental approach and a different normalisation procedure to obtain cross sections for (1) with much higher precision for electron impact energies ranging from about 15 to 4000 eV. Our measurements have been carried out using a pulsed crossed-beam technique in which, immediately after transit of a short duration pulse of electrons through a thermal energy target beam, the slow-ion collision products are swept out by a transverse electric field and selectively identified by their characteristic times of flight to a particle counter. This approach also avoids some of the possible uncertainties inherent in all previous experiments, in that the ionising collisions occur in the absence of both electric and magnetic fields.

Our method has been adapted from the crossed-beam coincidence technique previously developed (Shah and Gilbody 1981) in this laboratory for studies of the proton impact ionisation process

$$H^+ + H(1s) \rightarrow H^+ + H^+ + e \tag{2}$$

in the energy range 38–1500 keV and more recently (Shah *et al* 1987) in the range 9–75 keV. In this work, protons were arranged to intersect a thermal energy beam of highly dissociated hydrogen. Slow ions and electrons formed as collision products in the crossed-beam region were extracted by a steady transverse electric field and separately counted by particle multipliers. Product H^+ ions were selectively distinguished from background gas species by time of flight analysis. The required H^+ ions from the ionisation process (2) were distinguished from those arising from the charge transfer process

$$H^+ + H(1s) \rightarrow H + H^+ \tag{3}$$

by counting the H^+ ions in coincidence with the electrons from the same ionising events. Measured relative cross sections for (2) were normalised at 1500 keV to theoretical values based on the first Born approximation (Bates and Griffing 1953), a procedure believed to involve the smallest uncertainties.

In the present work, our apparatus was designed so that a pulsed proton beam could be easily substituted for the pulsed electron beam used in studies of (1). Our measured relative electron impact ionisation cross sections for (1) could then be normalised with high accuracy to known equivelocity proton cross sections at high velocities where (2) is dominant and, at low velocities, where (3) is dominant.

2. Experimental approach

2.1. General description

Figure 1 shows a schematic diagram of the crossed-beam arrangement and the electronics for signal recovery.

A pulsed beam of electrons from the electron gun was arranged to intersect (at right angles) a highly dissociated thermal energy beam of hydrogen in a high vacuum region ($\sim 2 \times 10^{-7}$ Torr). As in our previous ion impact studies, the hydrogen beam was produced by a tungsten tube furnace in a separate differentially pumped chamber. Slow H^+ ions resulting from (1) were extracted by an electric field applied between the high transparency grids G_1 and G_2, set into the conical electrodes C_1 and C_2 and recorded as individual pulses by the multiplier M. The extraction field was applied in pulses immediately after the transit of each electron pulse through the hydrogen

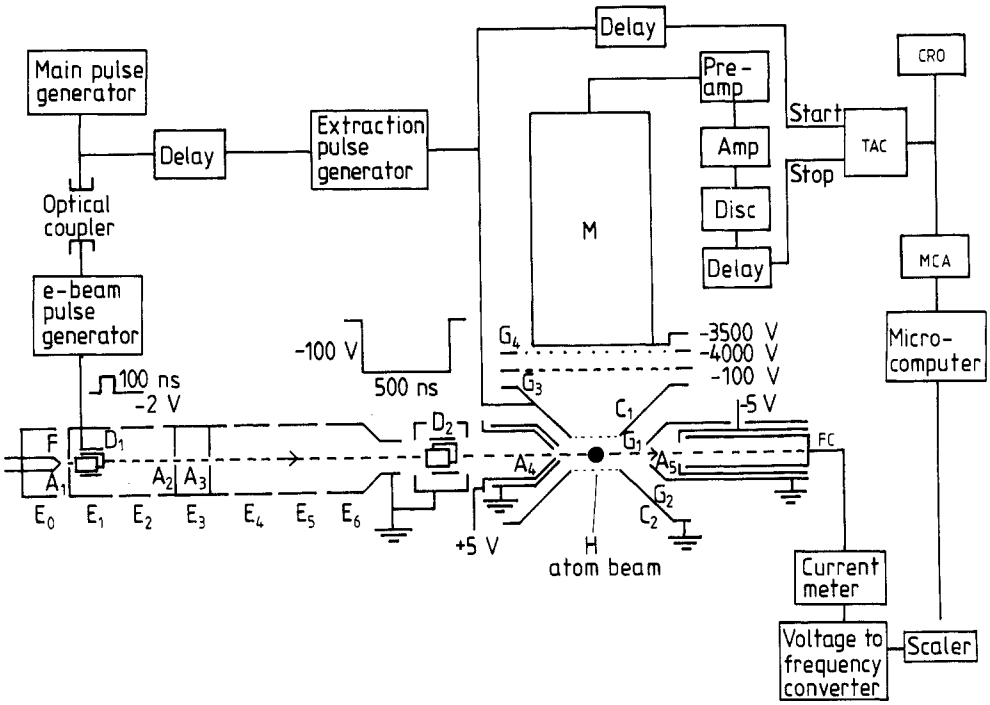

Figure 1. Scheme of experimental arrangement and electronics for signal recovery.

beam. The extracted ions could be identified by their different times of flight to the multiplier M in accordance with their charge to mass ratios.

The particle multiplier M was operated with the first dynode held at −3.5 kV. The grid G_4 in front of M was biased at −4.0 kV to prevent the escape of secondary electrons from the first dynode. A screening grid G_3 in front of G_4 was maintained at −100 V.

The final aperture A_4 of the electron gun was placed as close as possible (10 mm) to the centre of the H-atom beam, which was 4 mm in diameter in the region of overlap.

The final aperture A_4 of the electron gun was placed as close as possible (10 mm) to the centre of the H-atom beam which was 4 mm in diameter in the region of overlap. The absence of electric fields in this region during transit of the electron pulses ensured that the interaction volume remained constant, irrespective of the energy of the primary electrons. Care was taken to reduce stray magnetic fields to a very low value by surrounding the electron gun, extraction electrode assembly and the Faraday cup electron-beam collector FC by multiple layers of mu-metal foil.

The seven-element electron gun was based on the design of Crowe *et al* (1983) and Hollywood (1979) developed previously in this laboratory. The three cylindrical elements E_1, E_2 and E_3 form one set of lenses and elements E_3, E_4, E_5 and E_6 form a second set. A V-shaped filament F formed from 0.15 mm diameter thoriated tungsten wire was housed inside the element E_0 and two pairs of mutually perpendicular transverse deflector plates D_1 were housed within E_1. Elements E_0 and the midpoint of the filament were set at the same potential corresponding to the required electron energy. Element E_3 was held +300 V above E_0 while the potential of E_1 (0 to +20 V) was adjusted, together with the potentials of E_2 and the deflecting plates D_1, to give maximum transmission of the electrons through the apertures A_2 and A_3.

Having optimised the potentials of E_1, D_1 and E_2 at one energy, these remained unaltered throughout the entire energy range. It was only necessary to adjust the potentials of E_4 and E_5 of the second lens and the second set of deflector plates D_2 for different energies. In this way, the same intensity of the electron beam (typically about 0.1 μA) could be obtained throughout the 15-4000 eV energy range of our measurements. The apertures A_1, A_2 and A_3, which were 0.4, 0.25 and 0.5 mm in diameter respectively, ensured that the electron beam traversing the interaction region was not significantly divergent. The beam had a diameter somewhat smaller than that of the final aperture A_4. The electron beam finally passed through the 6 mm diameter aperture A_5 and was recorded by the Faraday cup FC in an assembly designed to suppress secondary electrons. Recorded currents were fed via a voltage to frequency convertor to a scaler.

In the interaction region the electron beam had a diameter not exceeding the 2 mm diameter of aperture A_4 while the diameter of the hydrogen beam was 4 mm. The effective collision volume was therefore not sensitive to the vertical position of the electron beam. This was checked by using the deflector plates D_2. The product ion signal per unit electron-beam intensity was shown to remain constant to within 1% for electron-beam deflections up to the maximum permitted by aperture A_4.

The tungsten tube furnace (figure 2) used in this experiment differed from that used in our previous ion impact studies (Shah and Gilbody 1981) since, in the present work with low energy electrons, it was important to minimise stray magnetic fields arising from the heating current. In the present design an inner tungsten tube 2 mm in diameter was supported by molybdenum spacers within a 4 mm outer tube. The heating current flowed in opposite directions in the two tubes thereby reducing the resulting magnetic field near the exit aperture of the furnace to a low value. The tungsten tubes were fabricated from 0.025 mm thick foil. With a heating current of about 45 A the temperature of the inner tube, into which the hydrogen gas was introduced at a constant rate, was maintained at 2600 K. The pressure in the surrounding region of the hydrogen furnace provided a convenient continuous indication of the intensity of the hydrogen beam during operation.

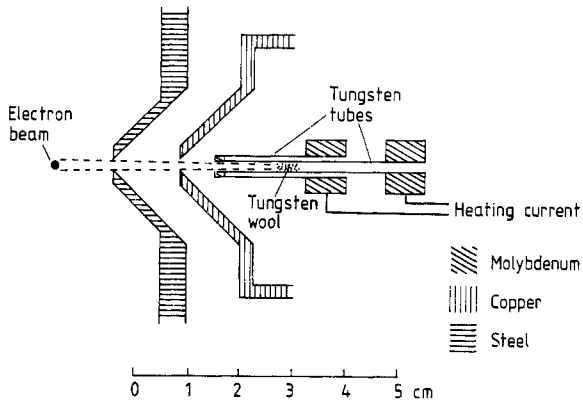

Figure 2. Arrangement of the tungsten tube furnace.

2.2. Electronics and signal recovery

The main pulse generator (figure 1), which produced pulses at 10^5 pps, was used to trigger the electron-beam pulse generator, which provided pulses of amplitude 2 V and

duration 100 ns. These pulses were applied to the deflection plate assembly D_1 to produce the pulsed electron beam. The electron-beam pulse generator was maintained at the required high potential by optical coupling to the main pulse generator through a 1 m long glass fibre link.

The extraction pulse generator, which was connected to grid G_1, was triggered by the main pulse generator via a variable delay which could be adjusted according to the transit time of the trailing edge of the electron pulse through the H-atom beam. Pulses of amplitude −100 V and 500 ns duration were found to be sufficient to collect all the slow-ion products of ionisation formed in the beam intersection region. In the worst possible case we estimate that, for average H-beam velocities corresponding to a furnace temperature of 2600 K, the H^+ ions formed through interaction with the leading edge of the electron pulse would drift a distance of only about 1 mm before the extraction pulse is applied. This distance was well within the 12 mm diameter of the grids G_1 and G_2.

On application of the extraction pulse to G_1, the ions produced during transit of each pulse of electrons were accelerated to the same energy and arrived at the particle multiplier M after flight times characteristic of their e/m ratios. The time to amplitude converter (TAC) operated with start pulses from the extraction pulse generator and with stop pulses from the particle multiplier provided time of flight spectra of the type shown in figure 3. This shows the portion of the spectra containing the H^+ and H_2^+ peaks of interest obtained with a highly dissociated hydrogen beam (furnace hot) and with a molecular hydrogen beam (furnace cold). The small rise in background pressure resulting from the dumping of the hydrogen beam in the vacuum chamber significantly enhances the H_2^+ peaks observed. The dissociation fraction is thus much higher than that indicated by the apparent ratio of peak heights even after allowing for the difference in velocities of the target species.

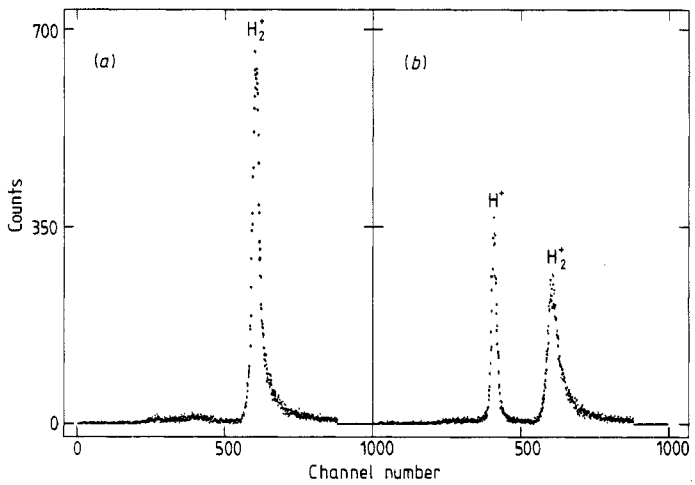

Figure 3. Time of flight spectra showing H^+ and H_2^+ products of ionisation with 98.2 eV electrons from (*a*) a molecular hydrogen beam with furnace cold and (*b*) highly dissociated hydrogen with furnace hot.

The timing of the extraction pulse applied to G_1 had to be carefully adjusted. This is illustrated in figure 4 which shows the dependence of the H^+ signal on the delay time for three primary-beam energies. Too long a delay after the transit of the electron

pulse results in incomplete collection of product ions and a fall in the H^+ signal. For too small a delay, the extraction pulse is applied before the electron pulse has traversed the H beam. The trailing portion of the electrons in the pulse will then tend to be

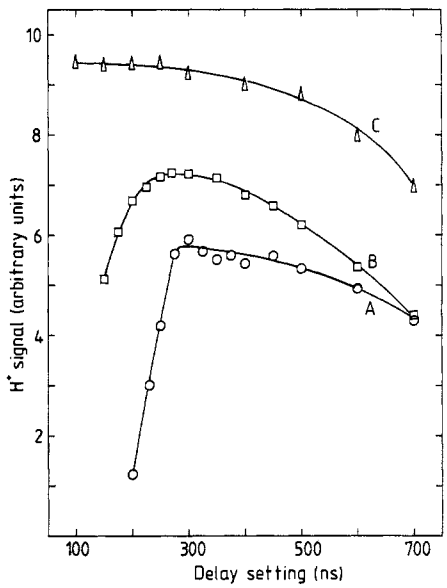

Figure 4. Dependence of H^+ signal on extraction pulse delay time (see text) at electron impact energies of 15.3 (A), 28.5 (B, ×0.2) and 1300 (C) eV.

deflected away before colliding with the H beam. This effect is illustrated by the results in figure 4 where the drop in H^+ signal for delay settings that are too low is greatest at the lowest electron energy. The optimum delay setting can be seen to decrease as the electron energy increases.

Recorded spectra from the multichannel analyser (MCA) were fed into a microcomputer which also recorded the electron-beam intensity and the signal from the hydrogen-beam monitor.

2.3. Cross section measurements and normalisation

Spectra for H^+ ion formation were recorded with the furnace operated at a low temperature when the hydrogen beam was entirely molecular and at a temperature of 2600 K when the hydrogen was highly dissociated. Allowance for a small contribution to the H^+ signal from dissociative ionisation of H_2 was made in the manner described previously in our proton impact studies (Shah and Gilbody 1981) by studying the temperature dependence of the H_2^+ signal. Unlike our previous proton impact work, which was carried out using a steady extraction field, the H^+ contribution from dissociative ionisation (see figure 3(*a*)) was very small in the present work. The initial velocity of formation of the H^+ products of dissociative ionisation is such that most of them escape from the extraction region before the extraction pulse is applied. Only those few ions with initial directions towards the multiplier will be recorded giving a very small but broadened peak.

Cross sections $\sigma_i(e)$ for the ionisation of H by electrons were obtained from the

expression

$$\sigma_i(e) = S/k\mu$$

where S is the H^+ signal per unit electron-beam intensity computed from the area under the appropriate peak in the time of flight spectrum; μ is the effective target density of the H atoms, a quantity related to the pressure recorded in the region surrounding the furnace, and k is the overall efficiency of H^+ ion detection which was found to remain constant over our full energy range.

In order to obtain absolute values of $\sigma_i(e)$ the product $k\mu$ was determined by reference to known proton impact cross sections. The electron gun (figure 1) was constructed on a sliding mount so that, within the vacuum chamber, a proton beam from a 10–100 keV accelerator could be easily substituted for the electron beam in precisely the same position with the target conditions unchanged. The proton beam was pulsed, by means of deflector plates in the beam entrance line, with the same mark to space ratio as the electron beam. With proton impact, H^+ product ions arise from both the ionisation process (2) and the charge transfer process (3). While (3) is negligible at high velocities, it provides the main contribution to H^+ formation for proton energies below about 30 keV.

In order to normalise the electron impact data, proton impact measurements were carried out in the range 12–75 keV using the sum of known cross sections $\sigma_i(p)$ and $\sigma_c(p)$ for (2) and (3) respectively. Values of (3) were obtained from the absolute

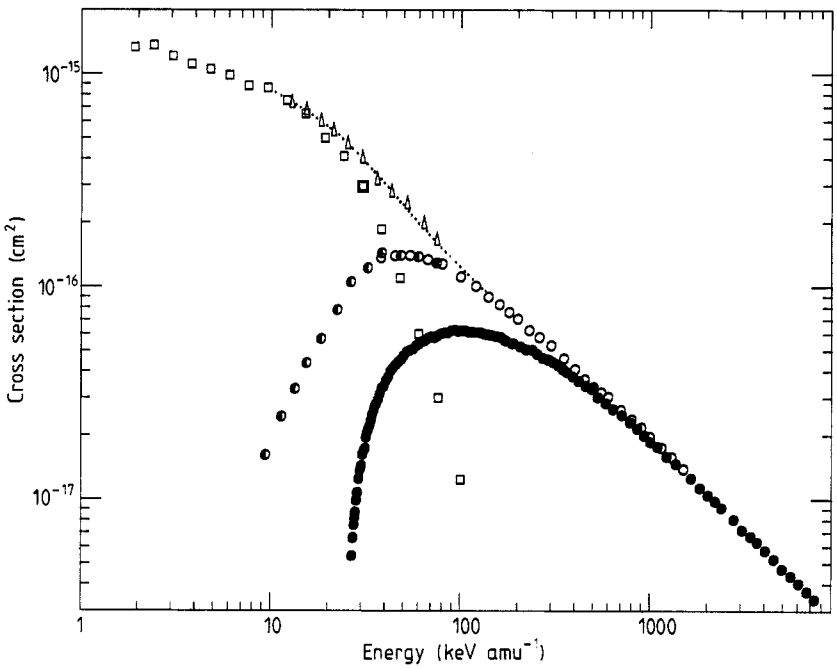

Figure 5. Equivelocity cross sections for H^+ production in collisions of protons and electrons with hydrogen atoms. ●, cross sections $\sigma_i(e)$ for electron impact ionisation in present work; ○, ◐, cross sections $\sigma_i(p)$ for proton impact ionisation (Shah and Gilbody 1981, Shah *et al* 1987); □, cross sections $\sigma_c(p)$ for proton impact charge transfer (McClure 1966); △, cross section sum $\sigma_i(p)+\sigma_c(p)$ for proton impact measured in present work; . . . , cross section sum $\sigma_i(p)+\sigma_c(p)$ with $\sigma_i(p)$ taken from ○, ◐ above and $\sigma_c(p)$ taken from □ above.

Table 1. Cross sections for electron impact ionisation of hydrogen atoms.

Energy (eV)	Cross section (10^{-17} cm^2)	Energy (eV)	Cross section (10^{-17} cm^2)
14.6	0.544 ± 0.025	63.0	6.14 ± 0.07
14.8	0.661 ± 0.041	66.0	6.11 ± 0.04
15.0	0.762 ± 0.038	69.0	6.11 ± 0.06
15.1	0.820 ± 0.029	72.1	6.01 ± 0.05
15.2	0.870 ± 0.045	75.5	5.96 ± 0.08
15.4	0.990 ± 0.046	79.5	5.91 ± 0.09
15.6	1.08 ± 0.03	84.0	5.84 ± 0.07
15.9	1.25 ± 0.05	89.0	5.78 ± 0.09
16.1	1.37 ± 0.06	94.0	5.59 ± 0.08
16.4	1.45 ± 0.05	102.0	5.40 ± 0.07
16.6	1.63 ± 0.03	103.0	5.42 ± 0.04
16.9	1.68 ± 0.06	113.0	5.23 ± 0.05
17.1	1.73 ± 0.05	121.0	5.07 ± 0.08
17.4	1.96 ± 0.06	130.2	5.05 ± 0.06
17.6	2.07 ± 0.05	138.2	4.83 ± 0.04
17.9	2.15 ± 0.05	148.2	4.62 ± 0.05
18.1	2.22 ± 0.06	158.2	4.55 ± 0.05
18.4	2.35 ± 0.03	168.2	4.43 ± 0.08
18.7	2.50 ± 0.06	178.2	4.28 ± 0.04
19.0	2.61 ± 0.04	188.2	4.10 ± 0.07
19.3	2.75 ± 0.05	198.2	3.98 ± 0.07
19.6	2.81 ± 0.04	213.2	3.79 ± 0.07
20.0	2.93 ± 0.09	228.2	3.61 ± 0.04
20.4	3.11 ± 0.10	248.2	3.43 ± 0.03
20.9	3.34 ± 0.02	268.2	3.31 ± 0.04
21.4	3.39 ± 0.04	288.0	3.03 ± 0.05
22.0	3.61 ± 0.05	317.9	2.84 ± 0.03
22.6	3.76 ± 0.09	347.9	2.66 ± 0.02
23.3	4.01 ± 0.06	387.9	2.50 ± 0.04
24.0	4.15 ± 0.06	427.9	2.31 ± 0.01
24.8	4.30 ± 0.10	467.9	2.15 ± 0.02
25.6	4.44 ± 0.10	508.2	2.00 ± 0.05
26.6	4.57 ± 0.10	548.2	1.86 ± 0.06
27.3	4.75 ± 0.07	598.2	1.77 ± 0.03
28.3	4.95 ± 0.09	668.2	1.59 ± 0.04
29.3	5.01 ± 0.06	748.2	1.47 ± 0.04
30.5	5.10 ± 0.05	818.2	1.38 ± 0.02
31.6	5.27 ± 0.07	898.2	1.26 ± 0.05
32.8	5.39 ± 0.08	998.2	1.13 ± 0.01
34.1	5.53 ± 0.03	1100.0	1.05 ± 0.01
35.4	5.59 ± 0.07	1200.0	0.982 ± 0.019
36.7	5.74 ± 0.05	1300.0	0.914 ± 0.015
38.1	5.83 ± 0.06	1506.7	0.807 ± 0.017
39.6	5.78 ± 0.07	1662.7	0.721 ± 0.023
41.2	5.89 ± 0.04	1848.1	0.673 ± 0.022
42.9	6.02 ± 0.07	1998.1	0.631 ± 0.020
44.7	6.07 ± 0.05	2198.1	0.577 ± 0.010
46.6	6.08 ± 0.09	2448.1	0.525 ± 0.012
48.6	6.23 ± 0.06	2698.1	0.472 ± 0.011
50.7	6.27 ± 0.08	2998.1	0.437 ± 0.021
52.9	6.19 ± 0.07	3298.1	0.403 ± 0.012
55.2	6.23 ± 0.05	3648.1	0.370 ± 0.006
57.6	6.21 ± 0.06	3998.1	0.339 ± 0.017
60.1	6.13 ± 0.10		

measurements of McClure (1966) while values of (2) were obtained from our previous measurements (Shah and Gilbody 1981, Shah *et al* 1987) in the range 9-1500 keV, which were normalised to theoretical values for proton impact based on the first Born approximation (Bates and Griffing 1953) at 1500 keV.

Our values of $\sigma_i(e)$ together with the present values of $(\sigma_i(p)+\sigma_c(p))$ and the previously measured cross sections $\sigma_i(p)$ and $\sigma_c(p)$ are shown in figure 5. The mutual consistency between the two sets of data can be seen to be very good with cross sections for equivelocity electrons and protons becoming equal at high velocities as expected on the basis of the first Born approximation.

Our values of $\sigma_i(e)$ are shown in table 1. The uncertainties associated with individual cross sections are assessed at the 67% confidence level and reflect the degree of reproducibility of the values in terms of the various experimental parameters and statistical fluctuations. An additional estimated uncertainty of 6.8% in the absolute values of $\sigma_i(e)$ is associated with our normalisation procedure.

2.4. Energy calibration

The collision energy of the electron beam can be expressed as $E = V_f - d$ where V_f is the potential of the midpoint of the V-shaped directly heated filament. The parameter d allows for the possibility that the apex of the filament did not coincide exactly with the midpoint and for the effect of contact potentials in the system. A value of $d = 1.9 \pm 0.2$ V was obtained by extrapolating the H^+, H_2^+ and He^+ ionisation yields down to their respective threshold values E_i of 13.60, 15.43 and 24.58 eV for H, H_2 and He beams respectively. In figure 6 we show results obtained for H^+ formation. No specific claim is made for the energy spread of our electron beam, but an indication that this is small is provided by the very small observed signals below threshold. This point will be mentioned again in § 3.

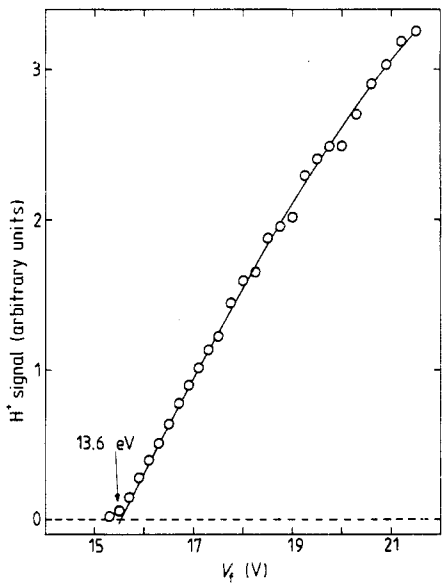

Figure 6. Dependence of H^+ yield on mid-filament potential V_f (see text) in collisions of electrons with highly dissociated hydrogen.

3. Results and discussion

In figure 7 measured cross sections $\sigma_i(e)$ for the electron impact ionisation of H may be compared with the previous experimental results of Fite and Brackmann (1958) and Rothe *et al* (1962) based on the modulated crossed-beam technique in the respective energy ranges 17–750 and 100–750 eV. Although the present results do not differ greatly from the data of Fite and Brackmann (1958) at the highest energies of overlap, at 750 eV the cross section measured by Rothe *et al* (1962) is about 20% lower than our value. At energies in the region of the cross section peak, there are significant differences between our results and those of Fite and Brackmann. For example, at 53 eV at the cross section peak, our value is 17% lower than that obtained by Fite and Brackmann.

In the region between about 25 and 30 eV, our values can be seen to overlap with those of Fite and Brackmann; at lower energies their values are considerably smaller. In this context, it is also interesting to compare the behaviour of our cross sections (figure 8) within a few eV of threshold with the measurements of McGowan and Clarke (1968). The latter were obtained using energy analysed electrons with a resolution less than or equal to 0.06 eV in a modulated crossed-beam experiment in which an RF quadrupole mass filter was used to select the product H^+ ions. Their measured cross sections are normalised to those of Fite and Brackmann (1958) at 23 eV. While the present results cast doubts on the accuracy of their normalisation, it is interesting to note the good agreement, especially in terms of energy dependence, between our results and those of McGowan and Clarke (1968) for energies up to about 20 eV. While the detailed structure of the threshold energy dependence of ionisation continues to be of

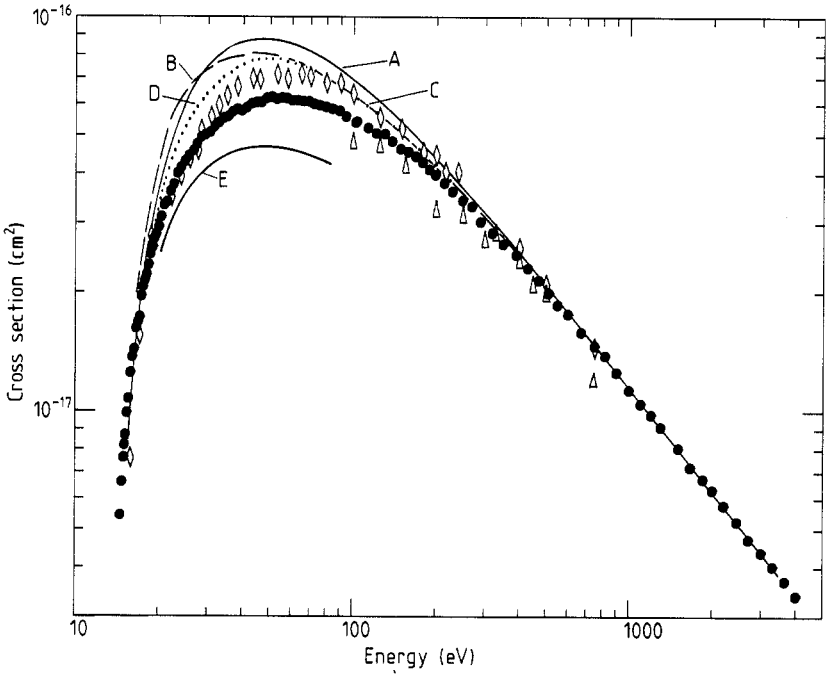

Figure 7. Cross sections for electron impact ionisation of hydrogen atoms. Experiment: ●, present work; ◇, Fite and Brackmann (1958); △, Rothe *et al* (1962). Theory: curve A, Born approximation (Peach 1986); curve B, Born approximation with exchange (Peach 1966); curve C, Born approximation with exchange (Mott and Massey 1965); curve D, Ochkur approximation (Peach 1986); curve E, pseudostate approximation (Gallaher 1974).

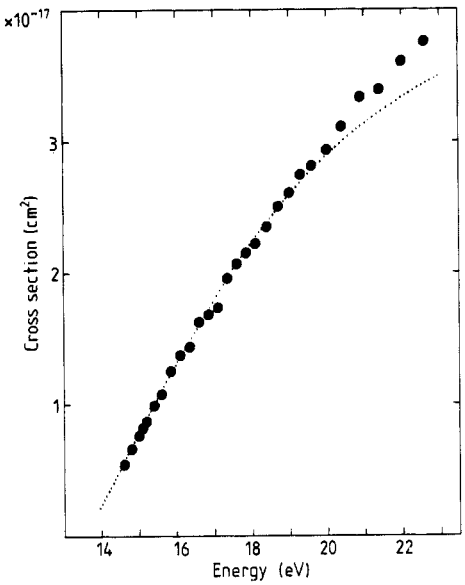

Figure 8. Near-threshold energy dependence of cross sections for electron impact ionisation of H atoms. ●, present results; · · · · · · · , McGowan and Clarke (1968).

considerable interest (see the recent discussion by Wetmore and Olson (1986)), in view of the fact that our energy resolution is unspecified and certainly poorer than that of McGowan and Clarke (1968), we do not address this question in the present work.

In figure 7 we include a number of theoretical estimates of $\sigma_i(e)$ based on different approximations. The values based on the first Born approximation calculated by Peach (1986) using improved numerical techniques but otherwise the same process as earlier calculations (Peach 1966), make no explicit allowance for exchange, but the direct amplitude includes contributions only from collisions where the energy of the ejected electron is less than that of the scattered electron. At our highest impact energies the Born values are in excellent agreement with our experimental values as expected on the basis of our discussion in § 2.3. At intermediate impact energies, the calculated values are up to 40% larger than our experimental values. Values calculated by Peach (1966) and Mott and Massey (1965) using the Born exchange approximation (figure 7) provide only slightly improved agreement with experiment in the region of the cross section maximum. A further small improvement in the agreement with experiment is evident in the case of values calculated by Peach (1986) using the Ochkur approximation which is a simplification of the Born–Oppenheimer approach (cf Peach 1966). We also include in figure 7 the results of calculations by Gallaher (1974) based on a 1s2s2p pseudostate. These values are seen to approach the experimental values only at low energies. The calculated values in the region of the cross section maximum are considerably smaller than experiment.

It is interesting to check the extent to which the present cross sections for H and the corresponding cross sections for the simplest isoelectronic ion He^+ conform to the simple scaling relation derived from the Thomson (1912) classical model of ionisation on the basis of which the cross section for ionisation of He^+ is expected to be only $1/Z^4 = \frac{1}{16}$ of that for H where Z is the atomic number. In figure 9 we plot $Z^4\,\sigma_i(e)$ against electron energy (in units of E/E_i) using the present cross sections for H and

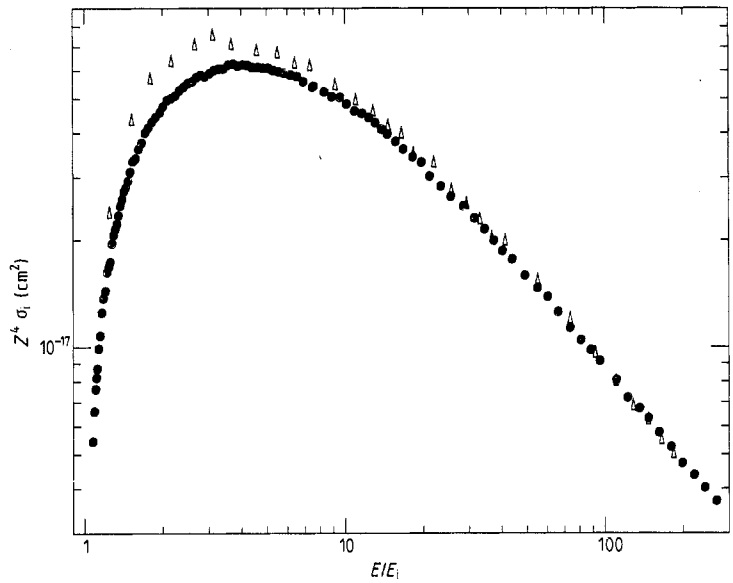

Figure 9. Classically scaled ionisation cross sections $Z^4\,\sigma_i(e)$ for electron impact ionisation of H and He^+ plotted against scaled energy E/E_i. ●, cross sections for atomic hydrogen (present results); △, cross sections for He^+ (Peart *et al* 1969).

the absolute values measured by Peart *et al* (1969) for He^+. The scaling relation is seen to describe the data well at energies E/E_i greater than about 10. At lower energies, the larger scaled cross section in the case of He^+, peaking at a lower energy than that for H, results from the effect of the acceleration of the incident electron in the Coulomb field of the nucleus.

At sufficiently high impact energies the electron impact ionisation cross section of an atom $\sigma_i(e)$ is described by the Bethe (1930) approximation and can be expressed in the form

$$\sigma_i(e) = A \log E/E + B/E \tag{4}$$

where

$$A = 2.303 \int_0^\infty \frac{df/d\varepsilon}{E_i + \varepsilon}\, d\varepsilon$$

with $df/d\varepsilon$ the continuous oscillator strength for the equivalent optical ionisation transition when the energy of the incident radiation is $E_i + \varepsilon$ and

$$B = -A \log(C_{nl}/4)$$

where C_{nl} depends on the particular atom. In the case of atomic hydrogen, Kingston (1965) has used the theoretical value of the continuous oscillator strength to calculate a value of $A = 1.30$. Calculation of the constant C_{nl} is more difficult, but Kingston (1965) has used the first Born approximation to derive C_{nl} for H, thereby obtaining a value $B = 2.92$. These values of A and B correspond to energies and cross sections expressed in atomic units.

Expressing (4) in the form

$$\sigma_i(e)E = A \log E + B \tag{5}$$

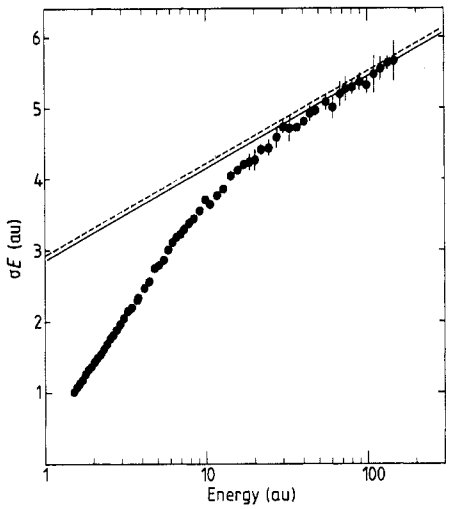

Figure 10. Bethe plot of $\sigma_i(e)\,E$ against $\log E$ for electrons in atomic hydrogen. ——, best fit of present data to Bethe expression; - - -, theoretical prediction (Kingston 1965).

we expect a plot of $\sigma_i(e)E$ against $\log E$ to exhibit a linear dependence at high velocities. In figure 10 our results when plotted in this way can be seen to be in excellent agreement with the theoretical prediction at our highest energies. The best straight-line fit through the data with a slope corresponding to $A = 1.30$ has an intercept corresponding to $B = 2.85$, a value only 2.5% lower than the value $B = 2.92$ calculated by Kingston (1965).

Acknowledgments

This project was supported by a research grant from the Science and Engineering Research Council. One of us (DSE) is indebted to the Department of Education, Northern Ireland for a Research Studentship. We are grateful to our colleague Dr A Crowe for information on the design of the electron gun used in these measurements. We are also grateful to Dr G Peach for sending us the results of calculations prior to publication.

References

Bates D R and Griffing G 1953 *Proc. Phys. Soc.* A **66** 961
Bethe H 1930 *Ann. Phys. Lpz* **5** 325
Crowe A, Nogueira J C and Liew Y C 1983 *J. Phys. B: At. Mol. Phys.* **16** 481
Fite W L and Brackmann R T 1958 *Phys. Rev.* **112** 1141
Gallaher D F 1974 *J. Phys. B: At. Mol. Phys.* 7 362
Hollywood M T 1979 *PhD Thesis* The Queen's University of Belfast
Kingston A E 1965 *Proc. Phys. Soc.* **86** 467
McClure G W 1966 *Phys. Rev.* **148** 47
McGowan J W and Clarke E M 1968 *Phys. Rev.* **167** 43
Mott N F and Massey H S W 1965 *Theory of atomic collisions* (Oxford: Clarendon) 3rd edn
Peach G 1966 *Proc. Phys. Soc.* **87** 381
—— 1986 Private communication
Peart B, Walton D S and Dolder K T 1969 *J. Phys. B: At. Mol. Phys.* **2** 1347

Rothe E W, Marino L L, Neynaber R H and Trujillo S M 1962 *Phys. Rev.* **125** 582
Shah M B, Elliott D S and Gilbody H B 1987 *J. Phys. B: At. Mol. Phys.* to be published
Shah M B and Gilbody H B 1981 *J. Phys. B: At. Mol. Phys.* **14** 2361
Tate J T and Smith P T 1932 *Phys. Rev.* **39** 270
Thomson J J 1912 *Phil. Mag.* **53** 449
Weigold E 1985 *Proc. 14th Int. Conf. on Physics of Electronic and Atomic Collisions, Palo Alto* ed D C Lorents, W E Meyerhof and J R Peterson (Amsterdam: North-Holland) invited papers p 125
Wetmore A E and Olson R E 1986 *Phys. Rev.* A **34** 2822